

BepiColombo - Correction of MERTIS Geometry. N. Schmedemann¹, H. Hiesinger¹, K. Wohlfarth², C. Wöhler², K. Bauch¹, M. D'Amore³, J. Helbert³, A. Maturilli³, A. Morlok¹, M. Reitze¹, A. Stojic¹, I. Weber¹, I. Varatharajan³ and the MERTIS Team, ¹Institut für Planetologie, Westfälische Wilhelms Universität, Münster, Germany (nico.schmedemann@uni-muenster.de), ²Image Analysis Group, TU Dortmund University, Otto-Hahn-Str. 4, 44227 Dortmund, Germany, ³Institute for Planetary Research, DLR, Rutherfordstrasse 2, 12489 Berlin, Germany.

Introduction: During the Earth flyby on April 10th 2020, the MERTIS instrument [1,2] on board the BepiColombo spacecraft successfully observed the Moon using its sideways oriented space baffle. Due to mechanical misalignment of the MERTIS instrument, the instrument pointing is different from its nominal position reflected in the instruments SPICE-Kernel [3] geometry. The lunar observation data of the MERTIS experiment revealed an offset of about 11.9 pixels in x-direction and about 1.5 pixel in y-direction (Fig. 1). We describe our approach to correct the observed misalignment.

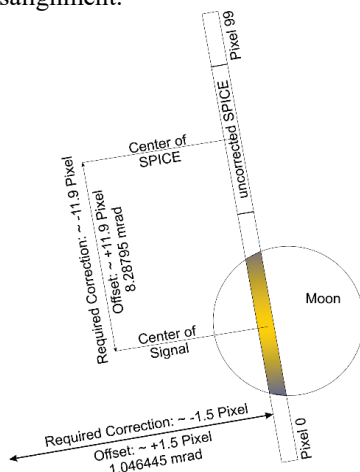


Fig. 1: Scheme of the MERTIS observation geometry for lunar observations during the Earth fly-by in April 2020.

Observation: The signal of the calibrated observation data shows an offset between the expected position of the lunar signal and the observed position of the signal (Fig. 2). This offset is not constant during the observation.

Geometric Correction: Assumptions made for geometry correction: In order to correct the misalignment of the observed signal with respect to the Spice-Kernel information we assume the following:

- 1) The sensor is misaligned in x-, y-, and z-direction.
- 2) The SPICE Kernel data for the spacecraft position and attitude are correct.
- 3) The detector misalignment can be corrected by adjusting x-, y-, and z-direction by minimizing the offset between signal and SPICE position on the detector for all frames of our lunar observation.

Approach for minimizing the offset between signal and SPICE position: To minimize the offset between signal

and SPICE position, for each frame that shows a signal, we identify the center of the signal and calculate the expected center of signal based on SPICE-Kernel data. The offset is variable during the lunar observation, indicating that the misalignment is not a simple offset along the spatial dimension of the sensor (x-direction) but a function of both x- and y-direction. The corrective offsets in x- and y- direction are found, if the corrected SPICE-Kernel geometry data is able to predict accurately the observed location of the signal on the sensor in all frames that show a signal.

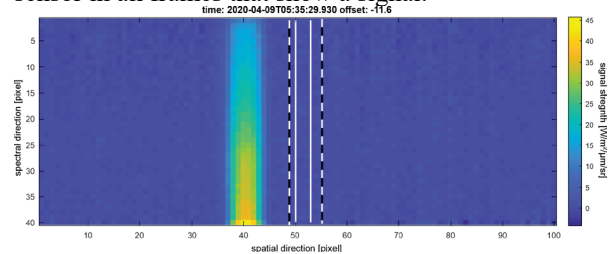


Fig. 2: Individual frame of the MERTIS instrument from the lunar observation. The vertical axis represents the spectral direction with a wavelength of $\sim 13.7 \mu\text{m}$ on the top and $\sim 7 \mu\text{m}$ at the bottom. The horizontal axis represents the spatial dimension with a pixel angular resolution of $\sim 0.7 \text{ mrad}$. Dashed vertical lines mark pixels that contain the lunar limb according to uncorrected SPICE-Kernel data. Pixel columns in and between solid vertical lines correspond to pixels that are completely contained within the lunar disk according to uncorrected SPICE-Kernel data. In the example the observed signal is offset by ~ 11.6 pixels towards smaller pixel numbers in the spatial dimension.

Detection of the center of signal: The center of the signal is determined by fitting a Gaussian to the signal cross section. For this approach, the signal is averaged along the spectral direction and fitted with a Gaussian along the spatial dimension (x-direction). The maximum of the fitted Gaussian is interpreted as the center of signal. Although this approach delivers subpixel accuracy, it is only the approximate center of signal, because at sufficiently high resolution, the signal pattern does not exactly follow a Gaussian pattern.

Determination of the predicted center of signal from SPICE-Kernel data: SPICE-Kernel data can be utilized to predict the location of the signal on the MERTIS sensor based on the given observation time, spacecraft position, and attitude as well as the instruments

orientation with respect to the spacecraft coordinate system. The ray vector in z-direction of the instrument coordinate system at the center of the sensor array is called “boresight”. The spatial extent of the sensor defines further ray vectors that define the sensor’s field of view. Based on SPICE-Kernel data it can be calculated which parts of the sensor will be covered by the observation target. As the sensor is made up of individual pixels, sufficiently dense calculation of spatially separated ray vectors allows for outlining the lunar limb within a single pixel and thus provides sub-pixel accuracy (Fig. 3). In order to provide sufficient sub-pixel resolution at reasonable computing times and comparable signal position accuracy, we chose a SPICE sub-pixel resolution of 21 by 21 sub-pixels within one physical pixel. This provides a 441 ray vector array for each physical pixel. Each of these ray vectors is tested to intersect with the lunar disk. If a pixel is completely contained inside the lunar disk all 441 ray vectors of a specific physical pixel hit the lunar disk. In the output shapefile we label such pixels accordingly with the variable “limb=0”. If for one physical pixel the number of sub-pixel ray vectors is 0 this pixel is completely outside the lunar disk and not recorded in our output shapefile. Any number of sub-pixel ray vectors in the range of 1 to 440 indicates that the physical pixel contains the lunar limb. Such pixels are indicated as “limb=1” in our shapefile output. The center of the predicted signal based on SPICE-Kernel data is thus determined from the pixels whose ray vectors hit the lunar disk.

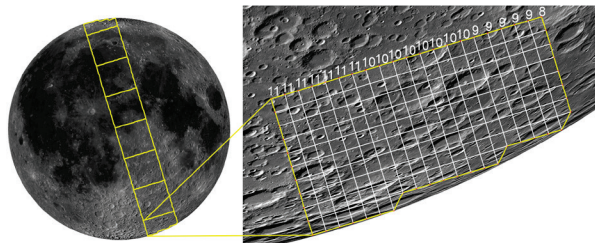


Fig. 3: Left: lunar disk (LROC-WAC Mosaic; [4]) as seen from spacecraft with pixel coverage of one frame. Pixels at the lunar limb are cut according to the sub-pixel resolution. Right: sub-pixel grid (white grid lines) of the limb-pixel at the southern lunar limb. White numbers indicate the number of sub-pixels between the northern pixel border and the lunar limb. The median of these numbers is used to calculate the fraction of the pixel that covers the lunar disk.

Minimizing the offset between predicted and observed position of the signal: For finding the correction values in x-, y-, and z-direction, we only change the amounts of the x and y offsets in the SPICE-Kernel data, since the value for z is defined by Eq.1.

$$(Eq.1) \quad z = \sqrt{1 - (x^2 + y^2)}$$

Starting with an angular correction for the MERTIS instrument of $x=0$ mrad and $y=0$ mrad, we measured the offset between the centers of the observed and predicted signal in 4929 frames from the lunar observation, which show a clear signal. The absolute value of the offset in each frame is summed up and compared to the result with different values for x and y. An optimization procedure [5] found a local minimum at $x=8.1071375$ mrad and $y=0.613725$ mrad offset. These values correspond to about 11.6 pixels offset in x-direction and 0.9 pixels offset in y-direction as each pixel is 0.7 mrad in height and length.

Remaining Error: The procedure outlined above assumes that the lunar disk is fully illuminated (phase angle=0°). However, the actual phase angle of the lunar observation was about 7.2° at the beginning of the observation and increased to about 8.7° at the end of the observation. Therefore, the radiance profile is not symmetrically distributed across the lunar disk but slightly shifted away from the lunar limb in shadow with slightly changing amount during the observation. For this reason, we refined the offset angles by fitting the observed radiance profile to a modelled radiance profile of the lunar disk [6].

Results: After two iterations with the radiance profile approach the pointing geometry was improved to a degree that continued parameter optimization did not improve the results any further. The final values for the offset of the MERTIS instrument with respect to its nominal orientation, rounded to the significant figures are 8.28795 mrad in x-direction and 1.046445 mrad in y-direction.

References: [1] Hiesinger, H., Helbert, J., 2010. The Mercury Radiometer and Thermal Infrared Spectrometer (MERTIS) for the BepiColombo mission. *Planetary and Space Science*, Volume 58(1), 144-165. [2] Hiesinger, H., Helbert, J., Alemanno, G. et al. Studying the Composition and Mineralogy of the Hermean Surface with the Mercury Radiometer and Thermal Infrared Spectrometer (MERTIS) for the BepiColombo Mission: An Update. *Space Sci Rev* 216, 110 (2020). <https://doi.org/10.1007/s11214-020-00732-4>. [3] Acton, C. H., 1996. Ancillary data services of NASA's Navigation and Ancillary Information Facility. *Planetary and Space Science*, Volume 44(1), 65-70. [4] Scholten, F., Oberst, J., Matz, K.-D., Roatsch, T., Wählisch, M., Speyerer, E.J., Robinson, M.S., 2012. GLD100 – the near-global lunar 100 meter raster DTM from LROC WAC stereo image data, *Journal of Geophysical Research*, 117, doi:10.1029/2011JE003926. [5] Lagarias, J. C., Reeds, J. A., Wright, M. H., Wright, P. E., 1998. Convergence Properties of the Nelder-Mead Simplex Method in Low Dimensions. *SIAM Journal of Optimization*. Vol. 9, Number 1, 112–147. [6] abstract 1241, this conference